Maneuver Acoustic Flight Test of the Bell 430 Helicopter

Michael E. Watts
NASA Langley Research Center

Royce Snider
Bell Helicopter Textron

Eric Greenwood
NASA Langley Research Center

Joel Baden
Bell Helicopter Textron

A cooperative flight test by NASA, Bell Helicopter and the U.S. Army to characterize the steady state acoustics and measure the maneuver noise of a Bell Helicopter 430 aircraft was accomplished. The test occurred during June/July, 2011 at Eglin Air Force Base, Florida. This test gathered a total of 410 data points over 10 test days and compiled an extensive data base of dynamic maneuver measurements. Three microphone configurations with up to 31 microphones in each configuration were used to acquire acoustic data. Aircraft data included DGPS, aircraft state and rotor state information. This paper provides an overview of the test.

Introduction

Airport congestion and flight delays continue to increase as passenger demand continues to grow. Vertical lift aircraft can have a significant impact on reducing airport congestion and flight delays. In 1995, the Civil Tiltrotor Advisory Committee Final Report to Congress (Ref. 1) found that CTR (Civil Tilt Rotor) could produce significant societal benefits, reducing airport congestion, creating jobs, and having a positive impact on the balance of trade. A study in 2001 (Ref. 2) showed that 26% of commercial operations from the 64 major airports had a trip length of less than 500 miles and could be offloaded from conventional aircraft with Runway Independent Aircraft. This resulted in a reduction of the projected 2017 average delay time from 86.5 minutes to 18.3 minutes, thus showing V/ESTOL aircraft can have a significant impact on commercial operations. An even more recent study (Ref. 3) focused on the three major regions of Atlanta, Las Vegas and the Northeast Corridor and found that a fleet of 90 and 120 passenger CTRs would reduce the average delays in 2025 from 60 minutes to less than a minute.

Several barriers need to be overcome before the public will accept rotorcraft for commercial scheduled operations. One of the barriers is the acoustic impact of these operations on the community in and around the terminal area. Rotorcraft noise heard on the ground is governed by three physical processes, as shown in Figure 1.

Noise from the rotorcraft is generated via several physical mechanisms across a range of frequencies and directions depending on the flight condition. This noise is then propagated through the atmosphere. The acoustic signal observed on the ground is affected by the atmospheric conditions and the terrain. Finally, the receiver perceives the signal in a way that is dependent on individual human characteristics.

Research testing, such as that reported in (Refs. 4, 5), has been performed by NASA and other agencies to gather data used to validate analytic acoustic codes such as the Rotorcraft Noise Model (RNM) (Ref. 4) that are designed to predict the noise footprint on the ground. However, these codes currently use steady linear segments for their flight paths. Previous testing has shown an acoustic impact when the helicopter turns (Refs. 6–8) or maneuvers aggressively (Ref. 9) but these data sets were either limited in scope or by poor weather conditions. A detailed set of maneuvering helicopter acoustic measurements is needed to better understand and incorporate these non-linear flight effects into ground footprint prediction codes.

Technical Approach

The NASA Langley Research Center (LaRC), Bell Helicopter Textron and the U.S. Army Aeroflightdynamics Directorate conducted a joint flight test to investigate the steady and maneuver acoustics of a Bell 430 helicopter, shown in Figure 2. This Maneuver Acoustic Flight Test was performed at Eglin AFB, Test Area B-75, in June/July 2011. The primary purpose for this flight test was to obtain a benchmark database of detailed acoustic source noise characteristics for a maneuvering helicopter. This database will be used to predict ground noise footprints due to vehicle operations, to develop low noise operations, and for the development and validation of acoustic prediction methods. Figure 3 shows the B-75 test range with the control area, reference locations and weather balloon systems indicated.

Presented at the American Helicopter Society 68th Annual Forum, Fort Worth, Texas, May 1-3, 2012.

Test Aircraft

The Bell Model 430 is an intermediate sized 10-place twin-turbine-engine helicopter incorporating a four-bladed main rotor and two-bladed tail rotor configuration. The engines are Allison 250-C40B turboshaft with Full Authority Digital Engine Control (FADEC). The main transmission is rated at 870 shaft horsepower for single engine operation (30 second rating) and 1311 shaft horsepower for twin engine operation. Maximum gross weight is 9300 pounds (4218 kilograms). Bell Model 430 specifications are shown in Table 1.

The acoustic test was conducted using Bell Model 430, S/N 49001 equipped with retractable wheel landing gear (Figure 2), owned and operated by Bell Helicopter Textron per experimental airworthiness certificate for research and development. The helicopter was externally configured as a standard Model 430 with the following exceptions: a flight test airspeed boom installed with angle of attack and angle of side slip vanes, NASA provided Tip-Path-Plane (TPP) data acquisition cameras mounted on the top of the left and right stub-wings, and small blade tracking tabs installed on the tips of the main rotor blades.

Aircraft Instrumentation

The aircraft was fitted with a customized version of the Micro Airborne Data Acquisition System (μADAS, Figure 4), including a Pilot Display Unit (PDU). The data acquisition unit portion of the NASA TPP system was mounted to the Bell Helicopter instrumentation pallet inside the cabin. Main rotor aircraft rigging was performed and documented prior to testing.

Accurate vehicle position data are essential to the generation of high-quality source noise semi-spheres. A Bell Helicopter Differential GPS (DGPS) system was installed on the aircraft for path guidance as well as an accurate measure of aircraft position. Aircraft mounted components of the DGPS included a GPS antenna, recorder, wireless modem and modem antenna. Additional aircraft components included instrumentation to process the base station correction signal, flight guidance processing and a pilot course deviation indicator (Figure 5). The ground station consisted of a precision GPS antenna located at a pre-surveyed location, a recorder and a wireless modem transmitter to broadcast the GPS correction signal to the aircraft (Figure 6). The desired guidance course was selected via the PDU and precision flight guidance cues were provided back to the pilot in real-time during flight test via the course deviation indicator.

The aircraft was instrumented with both collective and cyclic position measurement instrumentation as well as standard aircraft state parameters. Due to an under-voltage event that occurred while setting up the main rotor tip path plane system, several instrumentation cards were damaged. As a result of this and other set-up issues, not all instrumentation parameters were available during the entire test. A decision was made to perform each type of testing with minimum instrumentation required for that test phase. This decision allowed a gradual build-up of instrumentation during testing and reduced the programmatic risk.

The measurement of the main rotor tip path plane (TPP) angle-of-attack is desirable to accurately estimate the mean inflow through the rotor system and serves as an experimental check of theory for steady and quasi-steady flight. A TPP measurement system that accurately measures the location of the rotor tips at four locations around the aircraft was used during portions of this flight test. This system was developed for NASA by University of Maryland (UMD) and uses low powered lasers and cameras mounted on the aircraft as shown in Figure 7 (Ref. 10). These lasers are reflected off of reflective tape mounted on the rotor tips (Figure 8) and captured by the cameras at the four azimuth locations. The system was installed and operated on the aircraft by a Bell/UMD team.

An on-board aircraft attitude and rate gyro was used to provide pitch, roll and yaw attitudes and rates as a function of time. Analysis of the ships system attitude data indicated an intermittent and unpredictable drift in attitude signal. In an effort to obtain reliable aircraft attitude data, an Inertial Navigation Unit (INU) unit provided by the Army was installed during the maneuver portion of the testing. This unit recorded reliable pitch, roll and yaw attitudes and rates as a function of time. It should be noted that both the ships and Army INU systems provided consistent rate data, only the ships attitude data exhibited a drift. In spite of this intermittent problem, the ships system attitude data is useful in some cases when the INU data is unavailable to indicate abrupt changes in pitch, roll, and yaw attitude caused by pilot control inputs.

Table 2 lists the aircraft instrumentation installed, its accuracy and its availability during the different portions of the test.

Aircraft Data Processing

Following each test flight, the aircraft data were processed and downloaded using a mobile Bell Helicopter CAFTA (Computer Aided Flight Test Analysis) system. This enabled the test team to assess and validate aircraft state parameter and flight profiles performed during the same day of testing, prior to test planning for the next day.

Final processed and corrected aircraft data results were provided in the following format for each flight condition performed:

1. Two CAFTA output files with aircraft position and state parameter data sampled at 125 Hz,
2. One post-processed Track-file with all aircraft position and state parameter data in the CAFTA output files

down-sampled to the DGPS sample rate of five Hz and synchronized with UTC-time, and

3. One additional CAFTA output file with rotor once/rev azimuth reference sampled at 2000 Hz.

Microphone Instrumentation

The acoustic data were acquired using NASA's Mobile Acoustic Facility (MAF). This facility consists of two trailers used to control the flight test as well as maintain the 36 Wireless Acoustic Measurement Systems (WAMS) used to record the acoustic signals. Each WAMS consists of a ground board, microphone, GPS receiver and antenna. UTC time obtained from the GPS was used to synchronize all microphone, aircraft and weather information together. The WAMS setup used for this test consisted of a 1/2" Falcon (B&K 4189) microphone inverted 1/4" over a 15" round ground board, shown in Figure 9. The acoustic signals were acquired at 25,000 samples per second at 16 bit resolution. Up to 31 of these systems were deployed in three different configurations depending on the flight conditions being tested that day.

A recent upgrade to the WAMS system had the unforeseen consequence of introducing an intermittent delay of precisely one second to the recorded acoustic data. A procedure was developed to identify these delays and correctly synchronize the measured acoustic data. Using a previously developed time-domain de-Dopplerization technique (Ref. 11), the acoustic pressure time-histories for all recorded signals during each run were transformed from times of observation to times of emission. A window of the transformed data was then selected for each run when the helicopter was 3000 to 6000 feet before the microphones, such that the measured signal primarily reflected the thickness noise radiated by the main and tail rotors. A cross correlation of these windows was computed for all possible channel pair combinations in the array. The cross correlations were then used to uniquely identify the channels offset by one second. This is possible because the main rotor and tail rotor blade passing frequencies are non-integer multiples of each other, such that the period between phase alignment of the main and tail rotor thickness signals is much greater than one second.

Source Layout

Straight line level flight and steady descents were measured using a linear array consisting of 21 microphone locations in a 3,429 foot line perpendicular to the flight path. The spacing was set such that there was a microphone every 11.5°from directly below the aircraft to near inplane of the rotor for a flyover height of 150' above the center microphone. Three locations (directly below and +/- 45 degrees for 200' flyover altitude) had three microphone configurations; inverted 1/4 inch over a ground board, flush mounted in a ground board and on a four foot tripod. These three locations will provide data on the effects of elevating a microphone on a four foot tripod. The result was 27 microphones being deployed for this configuration. The source noise array is shown in Figure 10 and listed in Table 3 The coordinate center in the table is microphone 11 with positive x along the primary flight path, positive y to the left of the flight path and z is positive up. This array was also used for the steady turns portion of the test.

Maneuvering Layout

A 31-microphone array was designed to capture the likely BVI and near in-plane noise generated by the maneuvers to be flown when the aircraft was directly over the Maneuver Initiation Point (MIP) at 150 foot altitude. Figure 11 shows the resultant array, Table 4 lists the microphone locations in reference to microphone 34 which is the same location as microphone 11 in the source array. The coordinate system for this tabel is the same as that for the source layout. Figure 12 shows the projection of the microphones on an Lambert projection of the semi-sphere to illustrate the directivity pattern to be captured when the aircraft is directly over the MIP. The Lambert projection allows an undistorted picture of the external noise radiation pattern. The process of projecting the hemispherical surface as a 2D image using the Lambert projection is shown in Figure 13. The center of the plot, marked with an elevation angle of -90°represents the underside of the semi-sphere. The edges with a 0°elevation represent noise radiated in the horizon plane. Azimuth angles start at 0°behind the helicopter, and progress counterclockwise with the direction of the Bell 430 rotor rotation so that the right hand side of the plot represents the advancing side of the semi-sphere.

Terminal Area Layout

A microphone array was designed to capture approach noise for terminal area approach flight profiles. This array consisted of microphones placed primarily in a rectangular grid 3,000 by 6,400 feet and resulted in an array of 27 microphones. Figure 14 shows the resultant array and Table 5 lists the microphone locations relative to microphone 98 which is the same location as microphones 11 and 34. Note that the x direction is still along the flight path but that the primary flight path direction has changed. The Terminal Area Landing Point (TALP) is also listed in the table and shown on the figure.

Weather Instrumentation

An extensive set of weather measurements were made throughout the test. A tethered weather balloon system was located near the control area 0.9 miles from the reference microphone and continuously traversed from: 0 to 300 feet

during the source, steady turn and maneuvering flight portions; and 0 to 1000 feet during the terminal area approach testing. Another tethered balloon was placed 0.9 mile from the reference microphone and was stationary at a height of 300 feet. This stationary balloon had up to five weather sondes at constant altitudes during much of the test. Additionally, four weather sondes were placed on four foot tripods located amongst the microphone arrays and a sonde was mounted on a 30' pole. All weather sondes recorded wind speed and direction, temperature, pressure and relative humidity.

Flight Conditions Flown

Source Noise Mapping

Level Flight and Steady Descents Steady flight condition data were acquired for level flight and constant descent rate speed sweeps. These data are used to generate semi-spheres for the steady flight segments and are used by codes such as RNM for ground footprint prediction. Most of the level flight conditions were flown with the gear retracted and all descents were flown with the gear extended. Three days of source noise mapping flights were flown. Table 6 lists the nominal level flight conditions flown, the condition reference code and the number of points collected for that condition in the format L1 - 11 where L1 is the condition code and 11 is the number of data points acquired at that condition. All test condition tables in this paper use this format. Table 7 lists the constant descent flight conditions flown, the condition reference code and the number of points collected for that condition. An 80 knot, level flight housekeeping condition was flown during this portion of the testing to give an indication of the repeatability of the data. OASPL values as a function of distance along the flight track are shown in Figure 15 for seven runs spanning the three days of source noise mapping and shows a 3dB scatter when the aircraft was 850 feet in front of the center microphone.

The Blade Vortex Interaction Sound Pressure Level (BVISPL) is the integrated sound pressure level over the 5th thru 60th blade passage frequencies (116 to 1,392 Hz) and is used in the Lambert projection plots presented in this section as well as the contours presented in the Maneuvers section. Figure 16 presents noise levels during 80 knot level flight as measured and de-propagated to a 100-foot semi-sphere using an inverse propagation method accounting for spherical spreading, air absorption and ground effects. See (Ref. 4) for more information on this technique. Note that this frequency range includes tail rotor harmonics. Because there is little main rotor BVI noise in level flight the levels in this semi-sphere are set primarily by the tail rotor. Figures 17 to 19 show the 80 knot, 6°, 9°and 12°descent cases. It can be seen from these figures that the 9°case has higher BVI content and is radiated more towards the advancing side than the 6°case.

Steady Turns Steady level flight constant bank angle turns were flown over the linear source ground array. The helicopter approached parallel to the array and offset from the array line by the distance of the radius of the turn being flown. The turn was then initiated such that it was stabilized by the time a heading 45 degrees offset from the flight line was obtained with the goal to cross over the reference microphone. The pilot then maintained the designated angle of bank (15°or 30°) while simultaneously maintaining a constant airspeed of 60 or 80 KIAS at 200 foot AGL throughout the steady portion of the turn. The steady turn was held for at least 90 degrees of heading change with the aircraft exiting the turn parallel to the microphone array. This procedure for a right hand turn is shown in sketch form in Figure 20. Both left and right hand turns were flown with one test day devoted to acquiring steady turn data. The left and right turn flight paths are shown in Figure 21. Table 8 lists the conditions flown, the condition reference code and the number of points collected for that condition.Steady turns were flown with gear down.

Maneuvers

A primary focus of this test was acoustic characterization of maneuvers and five days of testing was devoted to these flight conditions. All dynamic maneuvers were flown with the gear down and were flown with slow, medium and fast control deflection rates. Nominally the fast rate was four times the slow rate and with the medium rate in between the slow and fast. The helicopter initially established a steady flight condition along a straight-line trajectory that is perpendicular to the primary linear array and passes over the Maneuver Initiation Point (MIP) which was 1500 feet before the reference microphone. This stabilized pre-maneuver flight condition was established approximately 500 feet before reaching the MIP. The pilot initiated the maneuver from the steady state flight condition just before reaching the MIP. The maneuver test plan focused on isolated control inputs such as cyclic pitch, cyclic roll and collective pull/push. More complex coordinated maneuvers were also acquired. Maneuver conditions were prioritized such that priority one acquired at least four points and priority two at least two points for each condition. An 80 knot level flight and 80 knot, fast cyclic pitch up at 6°descent (see Section Cyclic Pitch-Up below for a more detailed description) were chosen as housekeeping points and flown at the beginning and end of each flight. Figure 22 shows the OASPL, elevation over MIP and longitudinal cyclic control inputs for seven cyclic pitch up housekeeping points to demonstrate the consistency of the control inputs by the pilot and that the spread of acoustic data was within four dB.

Example data for each of the maneuver types are presented in the following sections. The pressure time histories were corrected for installation effects and then de-Dopplerized in the time domain. Three 4096 point FFTs

were performed centered around the time where the aircraft hub is over the MIP as indicated by the diamond in Figures 23 to 29. The BVISPL was then calculated and is presented as a contour plot of the noise footprint generated at this time of emission. The flight path in all maneuver plots is shown as a blue line with the aircraft moving from left to right. Also shown in each example are the cyclic and collective control positions and the roll and pitch attitudes. Longitudinal cyclic is 0% aft, lateral cyclic is 0% left and collective is 0% down. The 80 knot level flight baseline condition is shown in Figure 23. Maneuver conditions shown in Figures 24-29 are plotted likewise to demonstrate the change in acoustic radiation for each maneuver as compared to the steady level flight 80 knot condition.

Collective Pull-Up or Push-Over This maneuver was performed to measure the effect of a transient collective control input in isolation, starting from a level flight conditions where the wake is expected to be near the rotor plane. At the initiation of this maneuver, the pilot input a constant rate ramp input of collective pitch towards either the positive or negative, allowing flight path angle and airspeed to change freely. Only slow and fast maneuvers were executed based on emerging noise data indicating that the medium speed collective control inputs would yield little or no information. The maneuver was performed with cyclic control inputs primarily held fixed. The maneuver was initiated from level flight at 150 foot Above Ground Level at the MIP (AGLMIP) for positive collective pitch inputs and 250 foot AGLMIP for negative collective pitch inputs. Table 9 lists the conditions flown, the condition reference code and the number of points collected for that condition. Figure 24 shows a fast collective pull-up for 80 KIAS. This maneuver showed little change from the level flight baseline condition.

Cyclic Pitch-Up These maneuvers were performed to measure the effect of a transient longitudinal cyclic control input in isolation, starting from a level flight condition as well as a descending flight condition (6°and 9°descent angles) where the wake is expected to be near the rotor. At initiation of the maneuver, the pilot entered a constant rate ramp input of aft longitudinal cyclic, allowing flight path angle and airspeed to change freely. Slow, medium and fast cyclic control input maneuvers were executed, applying a longitudinal cyclic ramp input from a trimmed position towards the aft maneuver stop. All other controls were specified to be held fixed throughout the maneuver. The maneuvers were initiated at 150 foot AGLMIP for cyclic inputs initiated from level flight and 250 foot AGLMIP for maneuvers initiated from a descent. Table 10 lists the conditions flown, the condition reference code and the number of points collected for that condition. Shown in Figure 25 is a fast cyclic pitch-up initiated at 80 knots level flight and displays a significant increase in noise levels from either the baseline or the collective pull-up conditions.

Cyclic Roll These maneuvers were performed to measure the effect of a transient lateral cyclic control input in isolation. Cyclic rolls were started from a level flight condition as well as a 6°descending flight condition where the wake is expected to be near the rotor. At the initiation of the maneuver, the pilot entered a constant rate ramp input of lateral cyclic, allowing bank angle, flight path angle and airspeed to change freely. Slow, medium and fast control rates maneuvers were executed by applying a lateral cyclic ramp input at a rate defined as from trimmed position towards the left or right maneuver stop. All other controls were specified to be held fixed throughout the maneuver. Cyclic roll maneuvers were performed from stabilized conditions of level flight and 6°descent for 60, 80 and 100 knot indicated airspeeds. Level flight maneuvers were initiated at 150 foot AGLMIP for both left and right rolls. Descending maneuvers were initiated at 250 foot AGLMIP for both left and right rolls. Table 11 lists the conditions flown, the condition reference code and the number of points collected for that condition. Figure 26 shows a fast right roll initiated from 80 knots level flight.

Quick Stop/Start The quick stop/start maneuvers were flown to investigate the effect of the transition from steady constant airspeed flight to accelerating or decelerating flight. The onset of accelerating or decelerating flight changes the configuration of the rotor wake and has an effect on the radiated noise, especially during the transition to decelerating flight where the wake is expected to move closer to the rotor disk. The helicopter initiated the maneuver from a steady flight condition of 80 KIAS in level flight at 150 foot AGLMIP. The pilot began the acceleration or deceleration at 200 feet before the MIP using 2 kts/sec, 4 kts/sec and 6 kts/sec changes in airspeed along the flight path towards the target airspeed of 60 or 100 KIAS. Collective was controlled so that altitude was maintained during the maneuver. Table 12 lists the conditions flown, the condition reference code and the number of points collected for that condition. Figure 27 shows a medium rate deceleration initiated from 80 knots level flight.

Roll Angle Changes During Climbing Flight This maneuver is similar to the single control input cyclic descending roll maneuver, except that it is performed while the aircraft is climbing instead of descending. However, in order to initiate the roll maneuver at the desired altitude over the microphone array, the climb can only be entered just prior to the MIP. To perform this maneuver the helicopter started from steady level flight at 80 KIAS with an altitude of 150 AGLMIP. At 750 feet before the MIP, (2,250 Feet from reference microphone) the pilot began a 6°or 9°climb at constant airspeed. At the MIP the pilot performed a cyclic roll.

The roll rate was the same roll rate as the fast rate from the cyclic roll maneuvers and executed by applying a lateral cyclic ramp input from trimmed position to left/right maneuver stops. Table 13 lists the conditions flown, the condition reference code and the number of points collected for that condition. Figure 28 shows a right roll initiated from an 80 knot, 9 degree climb. For this condition, the aircraft altitude was 250 feet at the time of the contour as opposed to an altitude of 150 feet for the other example plots shown in the maneuvers section. This accounts for some of the reduction in noise seen when compared to Figure 26.

Roll Angle Changes During Accelerating Flight The rotor wake geometry is different in accelerating/decelerating flight than in steady flight, and provides a different initial condition for transient maneuvers. The purpose of these maneuvers is to assess the acoustic effect of decelerations or accelerations prior to entry into a turn. The helicopter initiated the maneuver from a steady flight condition of either 60 or 100 KIAS in level flight at 150 ft AGLMIP. The pilot then began to accelerate or decelerate at a rate of four kts/sec while maintaining 150 foot AGL. This acceleration or deceleration was initiated at a point such that the airspeed is approximately 80 KIAS at the MIP. Once the MIP is reached, the pilot performed a cyclic roll (left or right) while continuing to accelerate or decelerate. Table 14 lists the conditions flown, the condition reference code and the number of points collected for that condition. Figure 29 shows a right roll during a fast 100 to 80 knot deceleration.

Terminal Area Approaches

Terminal area approach data were acquired for verification of ground footprint predictions. A number of different approach profiles were flown ranging from simple constant speed, single descent angle to decelerating and turning approaches. All approaches were flown with gear down, started at 1000 foot AGL and terminated at the Terminal Area Landing Point (TALP) shown in Figure 14. The approaches are described below:

1. Single descent angle constant speed approaches were flown at 60 knots and angles of 6°(T1 - 2) and 9°(T2 -3). The airspeed was held constant during the descent until necessary to terminate the approach at the TALP

2. Single descent angle, decelerating approaches were flown starting at an airspeed of 100 knots and decelerating to approximately 20 knots at the TALP while holding 6°(T3 - 2), 9°(T4 - 2) or 12°(T5 - 2) descent angles.

3. Complex approaches that included multiple descent angles and multiple airspeed combinations were flown. Also flown were U-shaped and spiraling descents. Flying these complex approaches proved to be problematic and beyond the capability of the guidance system. Twelve attempts were made to fly the five complex approach profiles. These test points provide valuable information even though the actual profile flown varies from the defined profile since the aircraft information was recorded and can thus be used to predict the footprint for the actual profile flown and compared to the measured footprint.

4. Three test points were taken where the pilot was directed to fly the quietest profile possible based on his extensive piloting experience.

The measured Sound Exposure Level (SEL) contour for the A-weighted noise radiation during a standard 80 knot 6°approach is shown in Figure 30 and the contour for a 100 knot, 12°decelerating approach is shown in Figure 31. The higher speed, 12°, decelerating approach shows a significant decrease in SEL from the standard 6°approach and is the quietest approach profile flown during this test. This correlates with the observation made during the source noise measurements that the peak BVI descent rate is near 9°. This result is consistent with previous findings (Refs. 12–14) which show that during approach, deceleration at an angle steeper than the peak BVI condition can reduce noise.

Concluding Remarks

A cooperative flight test by NASA, Bell Helicopter and the U.S. Army to characterize the acoustics and measure maneuver noise on a Bell Helicopter 430 aircraft was accomplished during June, 2011 at Eglin Air Force Base, Florida. This test gathered a total of 410 data points over 10 test days and included extensive dynamic maneuver measurements. Three microphone configurations with up to 31 microphones in each configuration were used and specifically targeted to the acoustic data type being measured. Aircraft data were acquired that included DGPS, aircraft state and rotor state information. This data set contains a complete representation of the Model 430 aircraft for inclusion in the RNM data base. The example data shown in the maneuvers section demonstrate that maneuvers do lead to significant increases in noise. The maneuvers that involve using cyclic control inputs to change the pitch of the rotor tip-path-plane result in a particularly large increase in noise. The noise for this helicopter is relatively insensitive to collective inputs when started from level flight. This indicates that a good method of lowering noise when changing altitude is by primarily using collective inputs and minimizing rapid cyclic inputs. The terminal area measurements include a variety of flight paths ranging from simple to complex and provide valuable information for the validation of ground footprint prediction tools. This extensive data set is publicly available upon request.

References

[1]"CTRDAC-1995-REPORT, Civil Tiltrotor Development Advisory Committee Report to Congress in accordance with PL102-581," , December 1995.

[2]Johnson, J., Stouffer, V., Long, D., and Gribko, J., "Evaluation of the National Throughput Benefits of the Civil Tilt Rotor," NASA CR 2001-211055, September 2001.

[3]Chung, W. W. and et.al., "Modeling High-Speed Civil Tiltrotor Transports in the Next Generation Airspace," NASA CR 2011-215960, January 2011.

[4]Conner, D. A., Burley, C. L., and Smith, C. D., "Flight Acoustic Testing and Data Acquisition For the Rotorcraft Noise Model (RNM)," American Helicopter Society 62nd Annual Forum, May 2006.

[5]Watts, M. E., Conner, D. A., and Smith, C. D., "Joint Eglin Acoustic Week III Data Report," NASA/TM-2010-216206, March 2010.

[6]Greenwood, E., Schmitz, F. H., Gopalan, G., and Sim, B. W.-C., "Helicopter External Noise Radiation in Turning Flight: Theory and Experiment," American Helicopter Society 63rd Annual Forum, May 2007.

[7]Ishi, H., Gomi, H., and Okuno, Y., "Helicopter Flight Tests for BVI Noise Measured Using an Onboard External Microphone," AIAA Flight Mechanics Conference and Exhibit, San Francisco, CA, August 2005.

[8]Speigel, P., Buchholz, H., and Pott-Pollenske, M., "Highly Instrumented BO105 and EC135-FHS Aeroacoustic Flight Tests including Maneuver Flights," American Helicopter Society 61st Annual Forum, May 2005.

[9]Sickenberger, R. D., Gopalan, G., and Schmitz, F. H., "Helicopter Near-Horizon Harmonic Noise Radiation due to Cyclic Pitch Transient Control," American Helicopter Society 67th Annual Forum, May 2011.

[10]Sickenberger, R. D. and Schmitz, F. H., "Longitudinal Tip-Path-Plane Measurement using an Optics-Based System," American Helicopter Society 63rd Annual Forum, May 2007.

[11]Greenwood, E. and Schmitz, F. H., "Separation of Main and Tail Rotor Noise Ground-Based Acoustic Measurements Using Time-Domain De-Dopplerization," 35th European Rotorcraft Forum, September 2009.

[12]Lappos, N., Arnold, J., Erway, P., and McConkey, E., "The Development of a Decelerating Helicopter Instrument Landing system Using Differential GPS," American Helicopter Society 56th Annual National Forum, May 2000.

[13]Schmitz, F. H., Gopalan, G., and Sim, B. W.-C., "Flight-Path Management/Control Methodology to Reduce Helicopter Blade–Vortex Interaction Noise," *Journal of Aircraft*, Vol. 39, (2), 2002, pp. 193–205.

[14]Schmitz, F. H., Greenwood, E., Sickenberger, R. D., Gopalan, G., amd David Conner, B. W.-C. S., and III, E. M., "Measurement and Characterization of Helicopter Noise in Steady-State and Maneuvering Flight," American Helicopter Society 63rd Annual Forum, May 2007.

Acknowledgments

The test could not have been accomplished without a team of dedicated individuals. The test team consisted of three NASA, two Army, ten Bell, three Lockheed, two Air Force, one University of Maryland, and two Ole Miss personnel. Numerous NASA, Bell, UMD, Army and Air Force personnel also provided support before, during and after the test. The authors would like to thank their tireless effort, professionalism and dedication in making this test happen.

Figures

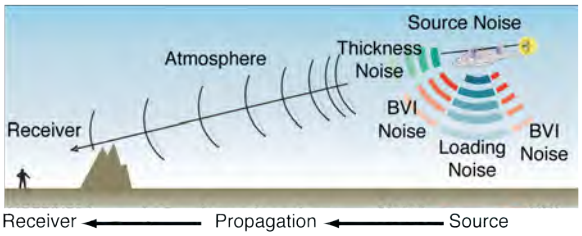

Fig. 1. Rotorcraft acoustics issues.

Fig. 2. Bell 430 helicopter.

Fig. 3. Testing area overview.

Fig. 5. Flight course deviation indicator.

Fig. 4. MicroADAS installation in aircraft.

Fig. 6. DGPS ground station setup.

Fig. 7. TPP cameras mounted on pylon.

Fig. 8. TPP reflective tape mounted on rotor tip.

Fig. 9. Wireless Acoustic Measurement System.

Fig. 10. Source noise microphone array.

Fig. 11. Maneuver microphone array.

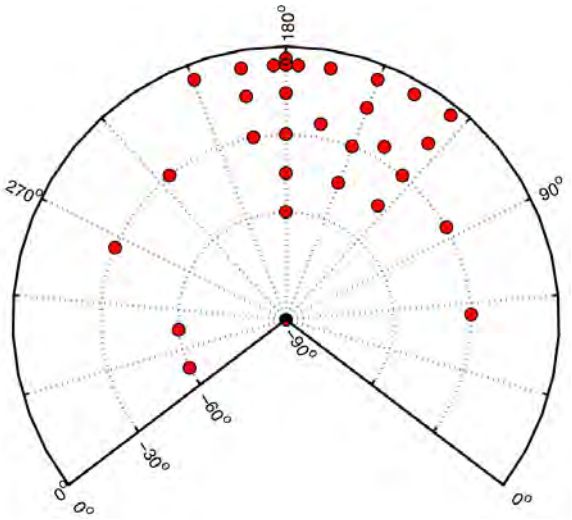

Fig. 12. Maneuver microphone array projection onto semi-sphere.

Fig. 14. Terminal area microphone array.

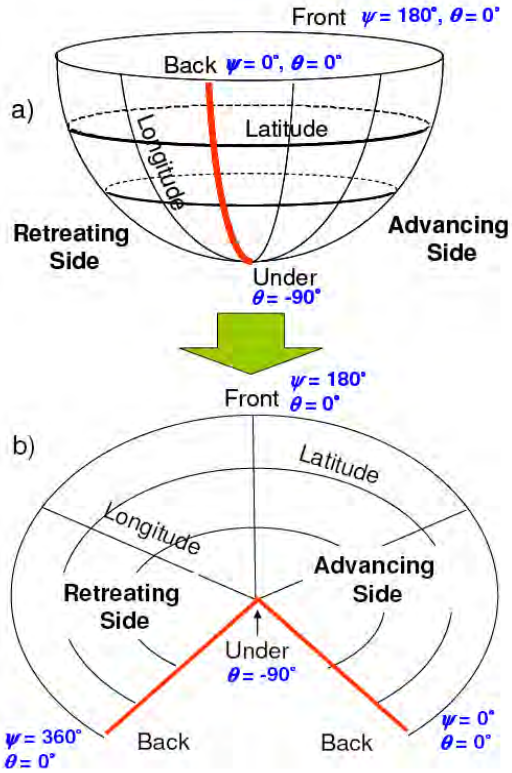

Fig. 13. Lambert conformal conic projection of an acoustic radiation semi-sphere.

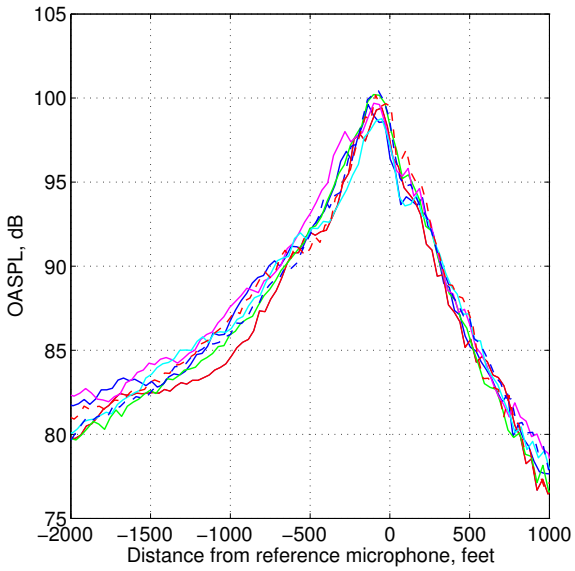

Fig. 15. Level flight, 80 KIAS housekeeping runs.

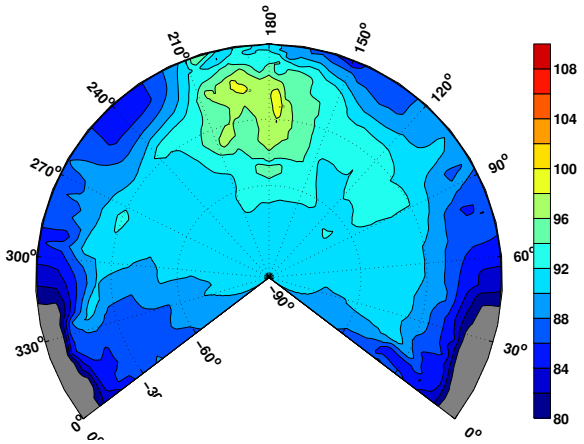

Fig. 16. Semi-sphere for 80 knots, level flight, BVISPL.

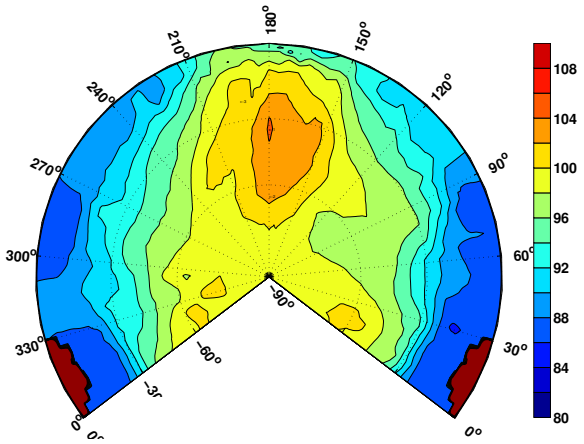

Fig. 17. Semi-sphere for 80 knots, 6°descent, BVISPL.

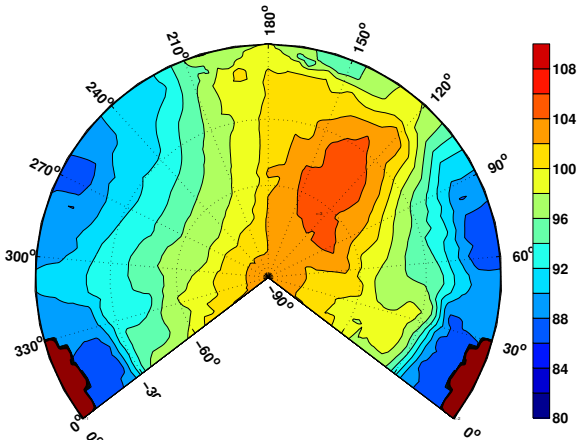

Fig. 18. Semi-sphere for 80 knots, 9°descent, BVISPL.

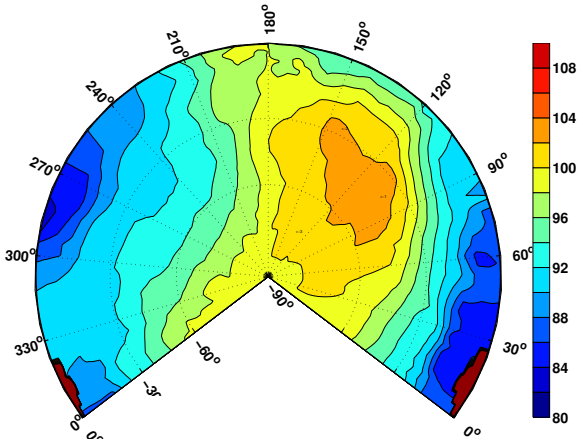

Fig. 19. Semi-sphere for 80 knots, 12°descent, BVISPL.

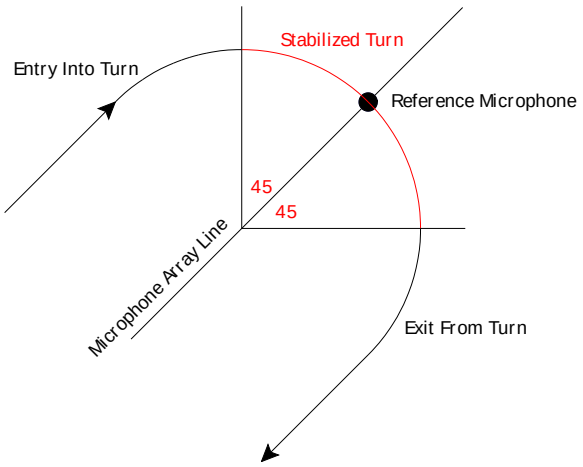

Fig. 20. Steady turn procedure sketch.

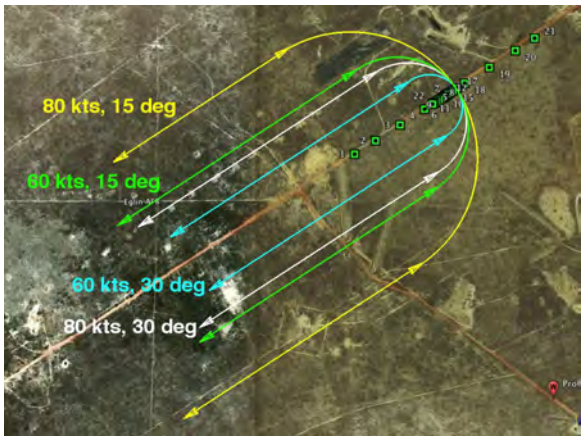

Fig. 21. Steady turn flight paths (radius is to scale).

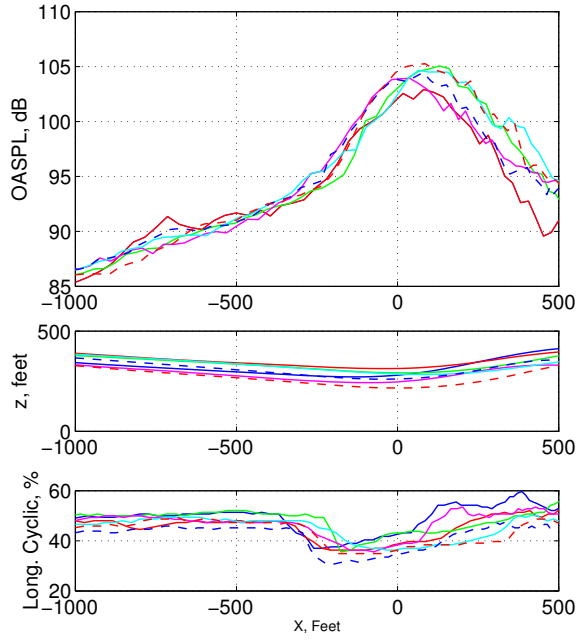

Fig. 22. Cyclic pitch up from 80 knot, 6 °descent house-keeping points.

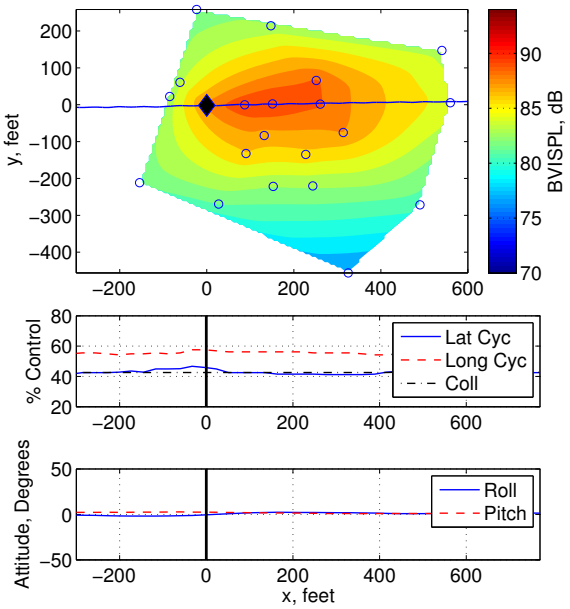

Fig. 23. Level flight, 80 knot baseline.

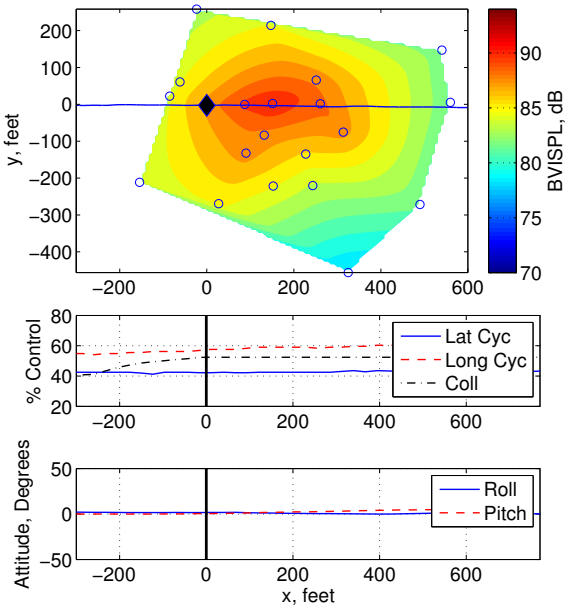

Fig. 24. Fast collective pull up at 80 knots.

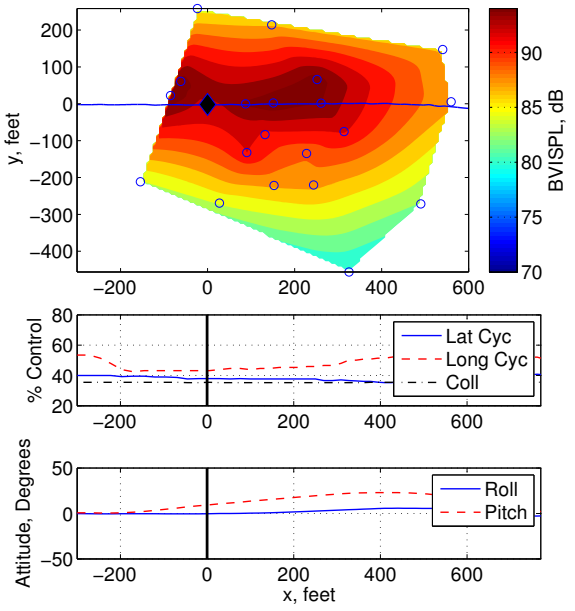

Fig. 25. Fast cyclic pull up initiated from 80 knots level flight.

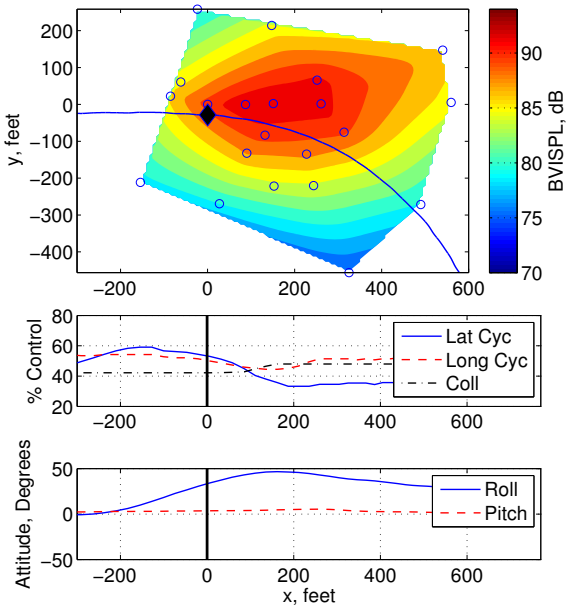

Fig. 26. Fast right roll initiated from 80 knots level flight.

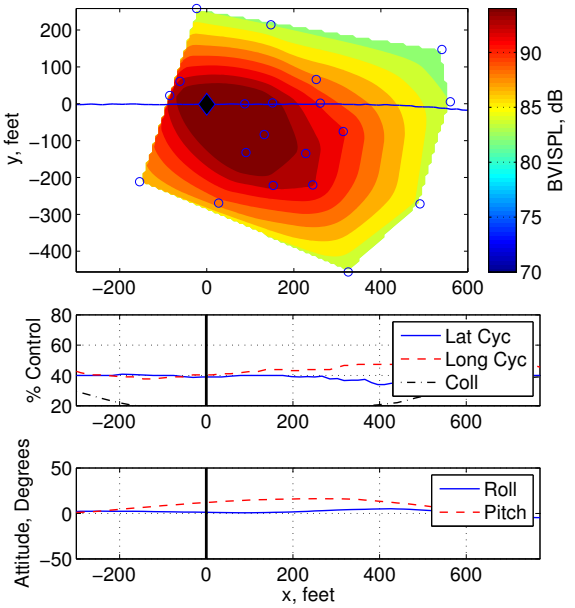

Fig. 27. Medium rate deceleration initiated from 80 knots level flight.

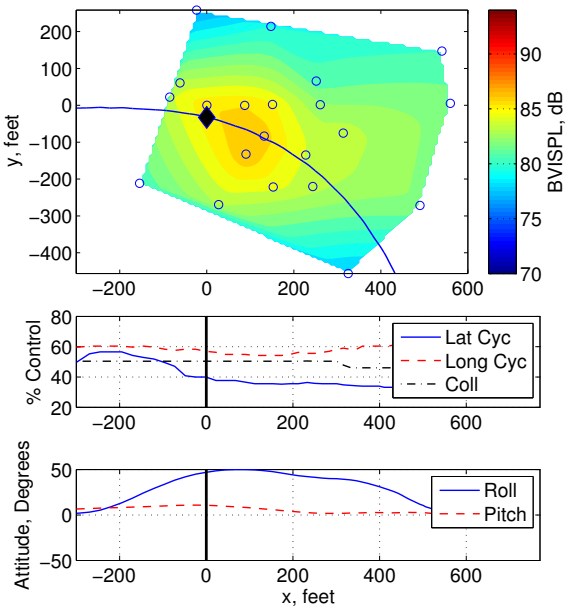

Fig. 28. Right roll during 9° climb.

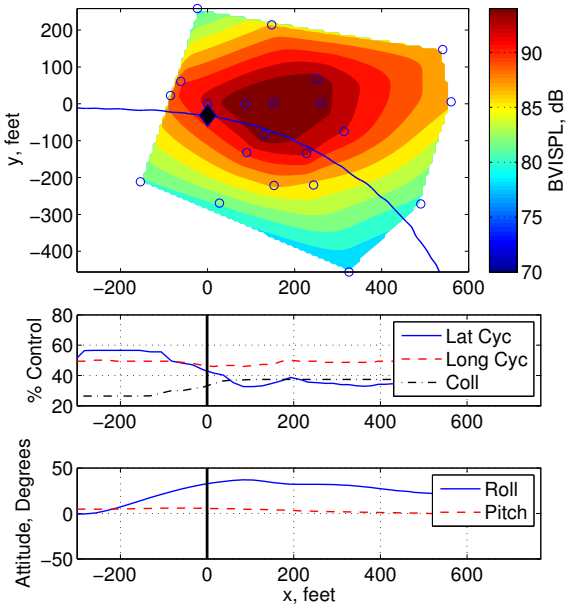

Fig. 29. Right roll during 100 to 80 knot fast deceleration.

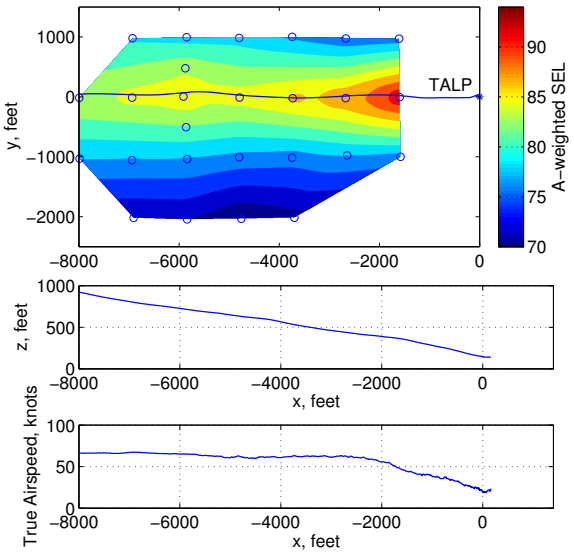

Fig. 30. Steady, 80 knot, 6°approach.

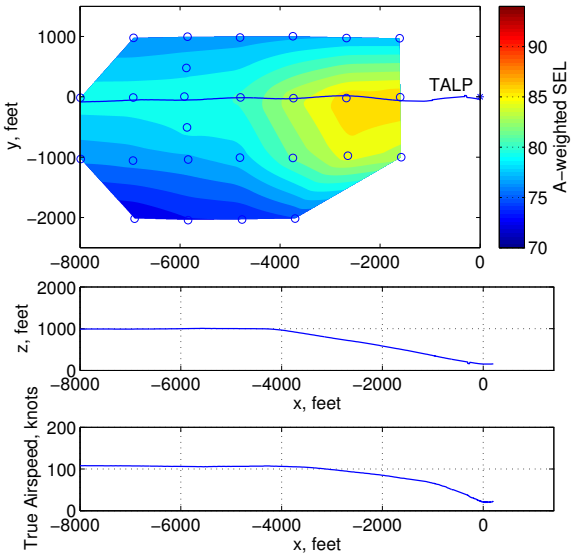

Fig. 31. Decelerating, 100 knot, 12°approach.

Tables

Table 1. Bell Model 430 Specifications

Main Rotor Diameter	42 ft
Num. Main Rotor Blades	4
MR RPM, BPF	348.6 RPM, 23.2 Hz
Tail Rotor Diameter	6 ft 10.6 in
Num. Tail Rotor Blades	2
TR RPM, BPF	1880.7 RPM, 62.7 Hz
Power Plant	2- Allison 250-C40B - 783 HP ea.
Empty Weight	5,305 lb
Max Take Off GW	9,300 lb
Max Speed	143 knots

Table 2. Aircraft Measurements

Sensor	Accuracy	Notes
Indicated Airspeed	+/- 2 knots	3, 4, 5
Static Pressure	+/- 0.5%	3, 4, 5
Dynamic Pressure	+/- 0.5%	3, 4, 5
Angle of Attack	+/- 0.5 deg	1, 3, 4, 5
Angle of Sideslip	+/- 0.5 deg	1, 3, 4, 5
Collective	+/- 2% range	3, 4, 5
Longitudinal Cyclic	+/- 2% range	3, 4, 5
Lateral Cyclic	+/- 2% range	3, 4, 5
Main Rotor Speed	+/- 0.5 RPM	3, 4, 5
DGPS Position	+/- 5 ft	2, 3, 4, 5
INU Roll/Pitch/Yaw Rate	+/- 5 deg/sec	4
INU Roll/Pitch Attitude	+/- 2.5 deg	4
Accelerations	+/- 0.01 g	2, 3, 4, 5
Torque	+/- 5%	6
Fuel Remaining	+/- 50 lbs	6
Tip Path Plane Angle	+/- 0.1 deg	7

1) Active during Portions of Source Testing
2) Active during All of Source Testing
3) Active during Steady Turn Testing
4) Active during Maneuver Testing
5) Active during Terminal Area Testing
6) Test Engineer notation, available during all testing
7) Active during part of Terminal Area Testing

Table 3. Source Array

Mic Number	x, ft	y, ft	z, ft
1	0.0	1714.6	13.7
2	-0.6	1319.2	15.0
3	0.3	850.4	16.2
4	-0.4	382.1	2.9
5	-2.0	232.7	0.6
6	-1.7	199.5	0.5
7	-1.6	155.9	-0.1
8	0.3	107.8	0.2
9	-2.5	63.1	0.4
10	-1.5	30.2	0.2
11 (ref)	0.0	0.0	0.0
12	-1.9	-28.1	-0.1
13	-1.9	-62.9	0.2
14	-1.7	-102.2	0.4
15	-2.0	-153.8	0.3
16	-2.0	-198.8	0.1
17	-2.8	-233.8	0.0
18	-3.5	-380.0	-1.1
19	-2.2	-850.5	-6.5
20	-2.6	-1349.0	-11.8
21	-1.9	-1714.3	-11.8
22 (1)	-1.7	199.5	0.5
23 (1)	0.0	0.0	0.0
24 (1)	-2.0	-198.8	0.1
25 (2)	-1.7	199.5	0.5
26 (2)	0.0	0.0	0.0
27 (2)	-2.0	-198.8	0.1

1) Microphone mounted flush in ground board
2) Microphone mounted on 4' tripod

Table 4. Maneuver Array

Mic Number	x, ft	y, ft	z, ft
30	675.9	-462.1	30.6
31	0.3	850.4	16.2
32	-0.4	382.1	2.9
33	0.3	107.8	0.2
34 (ref)	0.0	0.0	0.0
35	-1.7	-102.2	0.4
36	-3.5	-380.0	-1.1
37	-2.2	-850.5	-6.5
38	-2.6	-1349.0	-11.8
39	-3.1	-2153.1	-8.0
40	-942.0	1.3	-8.9
41	-960.0	143.5	-10.4
42	-1014.6	-274.8	-14.3
43	-1181.5	-457.6	-17.4
44	-1188.9	-76.7	-14.1
45	-1240.8	0.6	-13.3
46	-1249.4	64.9	-13.1
47	-1260.4	-220.9	-17.1
48	-1275.7	-135.5	-15.3
49	-1350.8	2.5	-14.0
50	-1352.2	214.4	-13.9
51	-1351.5	-221.2	-16.9
52	-1370.7	-83.2	-14.5
53	-1414.6	0.5	-14.3
54	-1413.1	-131.5	-15.1
55	-1477.3	-267.9	-16.9
56 (MIP)	-1501.8	1.7	-14.5
57	-1522.5	260.4	-13.1
58	-1562.8	63.0	-14.0
59	-1586.7	24.9	-14.2
60	-1658.6	-208.2	-14.3

Table 5. Terminal Area Array

Mic Number	x, ft	y, ft	z, ft
30	675.9	-462.1	30.6
70	-1869.7	-804.4	-15.0
71	-2925.3	-305.0	18.1
72	-1845.3	-286.5	3.2
73	-796.2	-298.8	1.1
74	261.4	-279.4	-8.7
75	1331.5	-308.5	-11.8
76	2395.9	-310.7	-0.5
77	-3987.6	-1298.0	15.4
78	-2932.2	-1294.6	11.0
79	-1908.1	-1277.6	-10.0
80	-787.8	-1292.4	-12.1
81	935.0	-950.2	-17.7
82	1331.1	-1302.9	-11.8
83	2406.2	-1288.0	-4.1
84	-3982.5	-2313.7	13.1
85	-2935.3	-2339.0	-7.5
86	-1832.3	-2321.2	-20.3
87	-796.7	-2289.6	-16.3
88	260.3	-2295.9	-9.4
89	1360.0	-2258.5	-10.3
90	2426.1	-2281.9	-7.4
91	-1855.2	-1788.7	-16.5
92	-2903.8	-3301.7	-23.5
93	-1833.9	-3326.5	-19.0
94	-754.3	-3315.8	-11.1
95	306.1	-3299.6	-14.4
96 (1)	935.0	-950.2	-13.9
97 (1)	1207.7	-1376.8	-14.9
98 (ref)	0.0	0.0	0.0
TALP	4004.4	-1281.8	-3.8

1) Microphone mounted on 4' tripod

Table 6. Source Level FlightsTest Points

KIAS	Gear Up	Gear Down
50	L2 - 1	
60	L3 - 5	
70	L4 - 2	
80	L1 - 11	L11 - 2
90	L5 - 1	
100	L6 - 2	
110	L7 - 1	L12 - 2
120	L8 - 3	
130	L9 - 5	

Table 7. Source Descent Flight Test Points

	Airspeed, KIAS				
Angle	50	60	70	80	90
-3°		A4 - 4		A18 - 2	
-6°	A2 - 3	A6 - 4	A13 - 3	A20 - 4	A27 - 2
-7.5°		A7 - 2	A14 - 1	A21 - 5	A28 - 1
-9°	A3- 1	A8 - 3	A15 - 2	A22 - 2	A29 - 1
-10.5°		A9 - 3		A23 - 3	
-12°		A10 - 3	A17 - 2	A24 - 2	

Table 8. Steady Turn Flight Test Points

		Bank Angle	
KIAS	Direction	15°	30°
60	Left	S1 - 2	S2 - 3
	Right	S5 - 6	S6 - 7
80	Left	S3 - 2	S4 - 7
	Right	S7 - 2	S8 - 11

Table 9. Collective Flight Test Points

		Rate	
KIAS	Input	Slow	Fast
60	PU	C1 - 2	C3 - 2
80	PU	C4 - 3	C6 - 6
	PO	C10 - 5	C12 -7

PU - Collective Pull
PO - Collective Drop

Table 10. Cyclic Pitch-Up Flight Test Points

		Rate		
KIAS	Angle	Slow	Medium	Fast
60	0°	D1 - 1		D3 - 6
	-6°	D7 - 2		D9 - 5
80	0°	D4 - 3	D5 - 2	D6 - 5
	-6°	D10 - 9	D11 - 2	D12 - 12
	-9°	D19 - 2		D21 - 2
100	0°		D22 - 3	D23 - 1

Table 11. Cyclic Roll Flight Test Points

			Rate		
KIAS	Angle	Input	Slow	Medium	Fast
60	0°	Left			R3 - 2
		Right			R15 - 6
	6°	Left			R9 - 2
		Right			R21 - 6
80	0°	Left	R4 - 5	R5 - 2	R6 - 7
		Right	R16 - 4	R17 - 2	R18 - 6
	6°	Left	R10 - 11	R11 - 2	R12 - 9
		Right	R22 - 6	R23 - 2	R24 - 11
100	0°	Right		R26 - 2	R25 - 2

Table 12. Quick Start, Quick Stop Flight Test Points

	Rate		
KIAS	Slow	Medium	Fast
80 to 100		M2 - 3	M3 - 5
80 to 60	M4 - 1	M5 - 4	M6 - 4

Table 13. Roll Angle Change During Climbing Flight Test Points

		Direction	
KIAS	Angle	Left	Right
80	0°to 6°	Z6 - 5	Z15 - 2
	0°to 9°	Z9 - 2	Z18 - 3

Table 14. Roll Angle Change During Accelerating/Decelerating Flight Test Points

		Cyclic Input	
KIAS	KIAS kt/sec	Left	Right
60 to 80	1	Y3 - 2	Y21 - 2
	2	Y6 - 5	Y24 - 4
100 to 80	-1	Y12 - 2	Y30 - 3
	-2	Y15 - 2	Y33 - 2